AD-A091 722 TUFTS UNIV MEDFORD MASS DEPT OF PHYSICS F/G 3/2
V.L.A. OBSERVATIONS OF SOLAR-ACTIVE REGIONS. I. THE SLOWLY VARY--ETC(U)
AUG 80 M FELLI, K R LANG, R F WILLSON F19628-80-C-0090
UNCLASSIFIED SCIENTIFIC-1 AFGL-TR-80-0225 NL

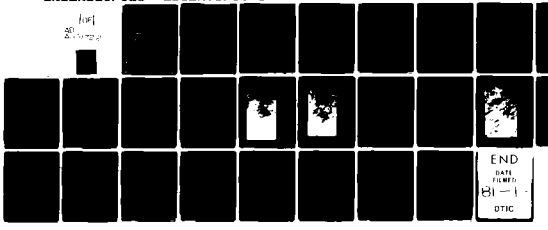

(18) AFGL-TR-80-0225 (19)

LEVEL II (12)

AD A091722

(6) V.L.A. OBSERVATIONS OF SOLAR-ACTIVE REGIONS. I. THE SLOWLY VARYING COMPONENT

(10) Marcello Felli
Kenneth R. Lang
Robert F. Willson

Department of Physics
Tufts University
Medford, Massachusetts 02155

(14) Scientific [redacted]-1

(12) 33

(11) 1 Aug [redacted]80

(15) F19628-80-C-0098 (16) 2311 (17) G3

Approved for public release; distribution unlimited

DTIC ELECTE NOV 20 1980 S D A

AIR FORCE GEOPHYSICS LABORATORY
AIR FORCE SYSTEMS COMMAND
UNITED STATES AIR FORCE
HANSCOM AFB, MASSACHUSETTS 01731

DDC FILE COPY

80 11 17 066

403317

Unclassified

SECURITY CLASSIFICATION OF THIS PAGE (When Data Entered)

REPORT DOCUMENTATION PAGE	READ INSTRUCTIONS BEFORE COMPLETING FORM
1. REPORT NUMBER: AF6L-TR-80-0225 / 2. GOVT ACCESSION NO.: AD-A091 722	3. RECIPIENT'S CATALOG NUMBER:
4. TITLE (and Subtitle): V.L.A. Observations of Solar-Active Regions I. The Slowly Varying Component	5. TYPE OF REPORT & PERIOD COVERED: Scientific Report No. 1 / 6. PERFORMING ORG. REPORT NUMBER:
7. AUTHOR(s): Marcello Felli, Kenneth R. Lang and Robert F. Willson	8. CONTRACT OR GRANT NUMBER(s): F 19628-80-C-0090
9. PERFORMING ORGANIZATION NAME AND ADDRESS: Department of Physics, Tufts University / Medford, MA 02155	10. PROGRAM ELEMENT, PROJECT, TASK AREA & WORK UNIT NUMBERS: 61102F 2311G3 BF
11. CONTROLLING OFFICE NAME AND ADDRESS: Air Force Geophysics Laboratory Hanscom AFB, Massachusetts 01731 Contract Monitor: Edward Cliver/PHP	12. REPORT DATE: 1 Aug. 1980 / 13. NUMBER OF PAGES: 33
14. MONITORING AGENCY NAME & ADDRESS(if different from Controlling Office)	15. SECURITY CLASS. (of this report): Unclassified / 15a. DECLASSIFICATION/DOWNGRADING SCHEDULE:

16. DISTRIBUTION STATEMENT (of this Report)

Approved for public release, distribution unlimited

17. DISTRIBUTION STATEMENT (of the abstract entered in Block 20, if different from Report)

18. SUPPLEMENTARY NOTES

This report has been submitted for publication in the Astrophysical Journal

19. KEY WORDS (Continue on reverse side if necessary and identify by block number)

Solar Radio Radiation, Very Large Array, Solar Corona, Active Regions, Magnetic Field, Polarization, Temperature, Bremsstrahlung, Electron Density, Plage

20. ABSTRACT (Continue on reverse side if necessary and identify by block number)

Very Large Array (V.L.A.) synthesis maps of the total intensity and the circular polarization of the active region AR 2032 at 6 cm wavelength are presented and compared with Hα photographs and Zeeman effect magnetograms of the same region with second-of-arc accuracy. The maps indicate that the radio emission is dominated by a small (≈ 30"), bright (10^6 K), circularly polarized (40% to 100%) source whose detailed morphological features are correlated with the chromospheric plage seen as bright regions on the Hα photographs. The large

DD FORM 1 JAN 73 1473 EDITION OF 1 NOV 65 IS OBSOLETE

SECURITY CLASSIFICATION OF THIS PAGE (When Data Entered)

20. (cont.)

brightness temperatures of the radio features indicate that they are the coronal counterparts of the chromospheric plage. The regions of enhanced emission at 6 cm wavelength exhibited substantial structural changes on a time scale of one day, and these changes were correlated with similar changes in the chromospheric plage. Weak or undetectable radio emission was found in the regions directly overlying sunspots; but two small ($\approx$ 10"), bright ($\approx 10^6$ K) radio sources were found at the outer edges of one sunspot where the magnetic field gradient is large. Although the degree of circular polarization varied from 40% to 100% in different regions of the dominant, plage-associated source, the entire source had one magnetic polarity and the general magnetic structure was correlated with the longitudinal magnetic field seen on magnetograms of the lower lying photosphere. This suggests that the 6 cm maps of circular polarization delineate the upward extension of the photospheric magnetic field into the low solar corona. Magnetic field strengths of between 450 and 900 Gauss are required at levels where the temperature exceeds a million degrees if the observed circular polarization is explained by either thermal bremsstrahlung or gyroresonance absorption. We interpret the observed radio emission of the bright plage-associated source in terms of the thermal bremsstrahlung of a hot (electron temperature $T_e \approx 2.5 \times 10^6$ K), dense (emission measure $\int N_e^2 dl \approx 2 \times 10^{29}$ cm^{-5} and electron density $N_e \approx 5 \times 10^9$ cm^{-3}) plasma. The spatial configuration, emission measure, electron density and temperature are all consistent with those inferred from X-ray observations of the coronal atmosphere above other active regions. The two small, bright radio sources found at the outer edges of one sunspot may be due to the gyroresonant absorption process, but this process is not the dominant radiation mechanism for this active region.

TABLE OF CONTENTS

		PAGE
A.	INTRODUCTION	5
B.	OBSERVATIONAL RESULTS	11
C.	THEORETICAL DISCUSSION	21
D.	CONCLUSIONS	22
E.	REFERENCES	31

A. INTRODUCTION

It has long been known that the slowly varying S component of solar radio emission, whose intensity is correlated with sunspot number and area, is connected with solar activity and has its origin in solar active regions. Early fan beam observations with angular resolutions of a few arc minutes, for example, led to the conclusion that the S component sources are located in the vicinity of both chromospheric plage and groups of sunspots; and because high brightness temperatures of $T_B \gtrsim 10^6$ K had been inferred for these sources they were attributed to enhancements in the density or temperature of the coronal atmosphere overlying active regions. Waldmeier and Müller (1950) and Waldmeier (1956) suggested that the S component is due to coronal condensations with an abnormally high electron density of $N_e \gtrsim 10^{10}$ cm^{-3}, while Piddington and Minnett (1951) reasoned that the condensations may also be abnormally hot with electron temperatures of $T_e \gtrsim 10^7$ K. Newkirk (1961) next used optical wavelength observations to derive a model for the enhanced electron density in the coronal regions above chromospheric plage and sunspot groups, and showed that this enhancement could account for the S component without modifying the coronal temperature from the value of $T_e \gtrsim 2 \times 10^6$ K which had been inferred from the Doppler broadening and the excitation of spectral lines. At this time the available data indicated that the S component is simply the thermal bremsstrahlung of the dense coronal condensations which overlay chromospheric plage or sunspot groups. A connection with intense magnetic fields had, of course, been suggested by the discovery that the radiation is circularly polarized (Covington, 1949); but this polarization could be easily interpreted in terms of propagation effects in which the extraordinary component of wave motion is enhanced in the presence of a magnetic field (Lehany and Yabsley, 1949; Denisse, 1950). In fact,

magnetic field strengths of $H \gtrsim 300$ Gauss could be inferred under the assumption that the thermal bremsstrahlung remains optically thin at a wavelength of about 5 cm where the circular polarization is about 30% (Gelfreich et al., 1959); while the low degree of circular polarization and the maximum brightness temperature of $T_B \gtrsim 2 \times 10^6$ K at the longer wavelength of $\lambda = 20$ cm could be explained by thermal bremsstrahlung which has become optically thick (Christiansen and Mathewson, 1959; Christiansen et al., 1960). By the late 1950's, then, the centimeter wavelength fan beam observations of the slowly varying S component could be interpreted in terms of the bremsstrahlung of thermal electrons in dense "coronal condensations", provided that intense magnetic fields are also present; but only the larger S component sources with angular sizes of $\theta \gtrsim 2'$ to 5' had been resolved in only one direction, and an alternative opacity source involving the acceleration of thermal electrons by magnetic fields had been overlooked.

Stepanov (1958) showed that the emission and absorption processes involving the gyroresonant radiation of thermal electrons accelerated by magnetic fields may compete with the processes involving the bremsstrahlung of thermal electrons accelerated in the electric fields of ions; and Ginzburg and Zheleznyakov (1959) showed that the gyroresonant absorption of radio waves could be important in the solar corona. Zheleznyakov (1962) then interpreted the slowly varying S component of solar radiation in terms of both thermal bremsstrahlung and gyroresonant radiation in a model involving gyroresonant absorption above sunspots and bremsstrahlung away from them. His core-halo model was based upon Kundu's (1959a, b) interferometric observations which showed that the S component sources at 3.2 cm contain an intense polarized core with an angular size $\theta \lesssim 1.8'$ surrounded by a weaker unpolarized halo whose angular extent ranges between 5' and 9'. The bright (10^6 K)

sunspot-associated cores, which were interpreted in terms of gyroradition at the second and third harmonics of the gyrofrequency, were thought to play an important role in the emission of solar flares, while the weaker 10^5 K halo emission was associated with the thermal bremsstrahlung of chromospheric plage. Additional support for this composite core-halo model with two radiation mechanisms was independently provided by Kakinuma and Swarup (1962) who showed that radiation at the gyrofrequency and its harmonics could explain the apparent peak in the spectrum of the S component at wavelengths λ = 6 to 12 cm, and that gyroresonant absorption produces circularly polarized radiation whose intensity decreases with increasing wavelength. Detailed core-halo models involving dipole magnetic fields, thermal bremsstrahlung at $\lambda < 5$ cm and $\lambda > 15$ cm, and gyromagnetic processes at 5 cm $< \lambda <$ 12 cm were subsequently developed by Lantos (1968), Zlotnik (1968a, b) and Zheleznyakov (1970). It soon became apparent, however, that the observations which had been used in support of these models could have led to misleading conclusions. The cores remained unresolved with only an upper limit to their angular size of $\sim$ 2'. This meant that the so-called core could be composed of smaller, brighter sources which might be associated with either sunspots or bright plage. Moreover, the dilution effects of observing these smaller sources with large antenna beamwidths would produce an artificial reduction in circular polarization which is unrelated to the emission mechanism of the radiation.

By the 1970's the development of high resolution radio wavelength interferometers and synthesis arrays, as well as the development of space instruments which detect solar X-ray and ultraviolet emission with high spatial and spectral resolution, led to a renewed interest in the competing models for the structure of the coronal atmosphere above solar active regions. Lang (1974a), for example,

used interferometric observations at a wavelength of λ = 3.7 cm with an effective angular resolution of 7" to show that the so-called core sources are actually composed of one or more bright sources with angular sizes of $\theta \tilde{\gtrsim} 20"$, brightness temperatures of $T_B \tilde{\gtrsim} 10^6$ K, and extraordinarily high circular polarizations of up to 100%. The presence of several bright components with angular sizes of about 20" and brightness temperatures ranging between 5×10^5 and 10^7 K was confirmed by interferometric observations at 2.8 cm wavelength (Felli, Pampaloni and Tofani, 1974; Felli, Tofani, Fürst and Hirth, 1975). Kundu and Alissandrakis (1975) next used the Westerbork Synthesis Radio Telescope (W.S.R.T.) at a wavelength of λ = 6 cm to resolve a solar active region into several discrete sources with brightness temperatures of $T_B \tilde{\gtrsim} 10^6$ K. They were able to show that the circular polarization of these smaller sources is as high as 90%, and that maps of the circular polarization correlate well with magnetograms of the longitudinal magnetic field in the lower lying solar photosphere. Subsequent analysis of the data by Kundu, Alissandrakis, Bregman and Hin (1977) suggested that the brightest components of the 6 cm emission are associated with sunspots, and this interpretation was used in support of calculations which indicated that the 6 cm radiation from solar active regions is predominantly due to the gyroresonant absorption process at the second and third harmonics of the gyrofrequency (Alissandrakis, Kundu and Lantos, 1980). Nevertheless, the W.S.R.T. data also indicated that intense 6 cm emission with $T_B \tilde{\gtrsim} 10^6$ K is associated with chromospheric plage where no sunspots exist. Very Large Array (V.L.A.) observations with higher angular resolutions and better positional accuracies will eventually determine if the newly resolved sources are predominantly associated with active region plage rather than sunspots,

and the observations presented here suggest that this may be the case.

The high degree of observed circular polarization indicates an intimate connection with coronal magnetic fields. Evidence for a correlation between the slowly varying component and the surface magnetic field of the Sun first come from eclipse and interferometer observations at centimeter wavelengths (Tanaka and Steinberg, 1964; Felli, Poletto and Tofani, 1977), as well as from single antenna observations at millimeter wavelengths (Kundu and McCullough, 1972). These observations indicated that regions of intense radio emission are associated with regions of enhanced magnetic fields seen on magnetograms of the lower lying photosphere. Synthesis maps obtained with the W.R.S.T. at 6 cm and 21 cm wavelength (Kundu, Alissandrakis, Bregman and Hin, 1977; Chiuderi Drago, Felli and Tofani, 1977) showed that the 6 cm maps of circular polarization have features which correlate well with the magnetograms, and that strong polarization can extend to the 21 cm level of the corona. Lang and Willson (1979, 1980) next showed that the shape, orientation and dipolar structure of 6 cm V.L.A. maps of circular polarization exhibit a marked correlation with similar features seen on photospheric magnetograms. Because the Zeeman effect magnetograms refer to the longitudinal component of the magnetic field, this correlation suggests that the circular polarization maps delineate the upward projection of the longitudinal magnetic field into the hotter coronal regions. Thus, the maps of circular polarization act as a coronal magnetogram, and for the first time it has become possible to delineate the magnetic field structure in the solar corona.

In this paper, we present V.L.A. synthesis maps of the active region AR 2032 at 6 cm wavelength, and compare them with Hα photographs and magnetograms of the same region with comparable angular resolutions and second-of-arc

positional accuracy. The synthesis maps given in Section II indicate that the radio emission is dominated by a small ($\tilde{\sim}$ 30"), bright (10^6 K), circularly polarized (40% to 100%) source whose morphological features are correlated with the chromospheric plage seen as bright regions on the Hα photographs. Weak or undetectable radio emission was found in the regions directly overlying sunspots; but two small ($\tilde{\sim}$ 10"), bright ($\tilde{\sim}$ 10^6 K) radio sources were found at the outer edges of one sunspot where the magnetic field gradient is large. Our observations are consistent with X-ray observations from rockets and the Skylab mission which indicate that a hot, dense plasma is contained within the arches of magnetic loops (Friedman, 1961, Landini, Fossi, Krieger and Vaiana, 1975; Vaiana, Krieger, Timothy and Zombeck, 1976; Vaiana and Rosner, 1978). The 10^6 K X-ray emission lies above extended regions of bright plage, while weak or undetectable X-ray emission is found directly over sunspots. The X-ray evidence suggesting cooler or more tenuous regions in the coronal atmosphere above sunspots is also consistent with E.U.V. observations which suggest that high columns of cool material project upwards to heights of $\tilde{\sim}$ 10^5 km from cool loops connected to sunspots (Foukal, 1975, 1976). Our synthesis maps of the circular polarization of AR 2032 indicate that the bright plage-associated source has one dominant magnetic polarity with a magnetic structure which is correlated with the longitudinal magnetic field seen on magnetograms of the lower lying photosphere. The brightest radio source therefore contains an intense magnetic field associated with the underlying plage but it does not seem to be directly associated with the magnetic field of the individual sunspots. In Section III we provide a theoretical discussion in which we interpret the brightest radio emission at 6 cm

wavelength in terms of the thermal bremsstrahlung of a hot (electron temperature $T_e \tilde{\sim} 2.5 \times 10^6$ K), dense (emission measure $\tilde{\sim} 2 \times 10^{29}$ cm^{-5} and electron density $N_e \tilde{\sim} 5 \times 10^9$ cm^{-3}) coronal condensation. The spatial configuration, emission measure, electron density and temperature are all consistent with those inferred from X-ray observations of the coronal atmosphere above other active regions. In Section III we also show that the high degree of circular polarization of the bright radio source requires an intense magnetic field strength of H = 450 to 900 Gauss at levels where the temperature exceeds 10^6 K. We also discuss the gyroresonant absorption process which predicts intense emission at large angles away from magnetic fields, and which is confined to a thin layer of $\tilde{\sim}$ 500 km thickness. Although gyromagnetic processes may account for the two small sources seen at the edges of one sunspot, the dominant plage-associated radio emission is due to bremsstrahlung from the hot, dense gas which is known to overlay the thin gyroresonant layer; and this interpretation is consistent with the association of intense radio emission with magnetic fields directed along the line of sight. In Section IV we summarize our basic conclusions.

B. OBSERVATIONAL RESULTS

We have used the Very Large Array (V.L.A.) to observe the active region AR 2032 on October 5 and 6, 1979. The position of AR 2032 on the Sun's surface was 17° N and 61° E at 13^h U.T. on Oct. 5, and 16° N 45° E at 13^h U.T. on Oct. 6. The V.L.A. was divided into two sub-arrays to give nearly

identical u-v coverage at two wavelengths λ = 6 and 20 cm. The λ = 6 cm sub-array was composed of 10 antennae with distances from the array center ranging between 0.04 and 5.72 km. The λ = 20 cm sub-array was composed of 9 antennae with distances from the array center ranging between 0.9 and 17.2 km. The individual antennae have a diameter of 25 m which provided respective beamwidths of 9' and 29' at λ = 6 cm and 21 cm. The average correlated flux of 45 interferometer pairs at λ = 6 cm and 36 interferometer pairs at λ = 20 cm was sampled every 30 s for both the left hand circularly polarized (LCP) and the right hand circularly polarized (RCP) signals. These data were then calibrated, edited and averaged to make synthesis maps of the total intensity I = (LCP + RCP)/2 and V = (LCP - RCP)/2.

The data were calibrated by observing 3C 273 for 5 min every 30 min, and by assuming that the flux density of 3C 273 is 35.14 and 20.5 Jy, respectively, at λ = 6 cm and 20 cm. The amplitude and phase of the observed data were calibrated according to the procedures described by Lang and Willson (1979) together with a correction for a difference in the temperatures of the switched noise source of each polarization channel. Solar flares, bad antennae, and interference were then edited from the data, but the u-v coverage at λ = 6 cm remained good and uniform. Because the individual antennae beamwidth at λ = 20 cm included the entire Sun, however, the 20 cm data were contaminated by five solar flares lasting up to an hour each. Because of contamination by solar flares, as well as calibration and confusion problems, we were unable to obtain accurate synthesis maps at λ = 20 cm; and for this reason we present the much more definitive results obtained at λ = 6 cm. The calibrated amplitude and phase of the 6 cm data

for each polarization and every antenna pair were taken to be the amplitude and phase of the source visibility function; and the source intensity distribution was then obtained by Fourier transforming the calibrated data and using the "clean" procedure on roughly 10,000 u-v components for each day of observation.

The data obtained during the daylight observing hours on Oct. 5 and 6 were used to obtain a synthesis map of the total intensity, I, for each day (Figure 1). Here the contours mark levels of equal brightness temperature corresponding to 0.1, 0.2....0.9, and 1.0 times the maximum brightness temperature $T_B(max)$; and the major and minor axis of the synthesized beam pattern are denoted by the cross marks in the upper left hand corner of the figure. Assuming a constant brightness temperature distribution over the synthesized beam area, Ω_B, we have $T_B(max) = 1.95 \times 10^6$ K with $\Omega_B = 37.98$ square seconds of arc on Oct. 5, and $T_B(max) = 2.50 \times 10^6$ K with $\Omega_B =$ 27.49 square seconds of arc on Oct. 6. This suggests that the brightest features of the enhanced radio emission have become optically thick with a brightness temperature equal to the electron temperature in the coronal atmosphere; and that the larger part of the enhanced radio emission comes from optically thin coronal regions with optical depths $\tau = T_B/T_e \lesssim 1$. [Continuum observations at X-ray wavelengths (Vaiana and Rosner, 1978), as well as the observed Doppler broadening and excitation of spectral lines at optical wavelengths (Newkirk, 1961), indicate that the coronal condensations above active regions have electron temperatures of $T_e = 2$ to 4×10^6 K].

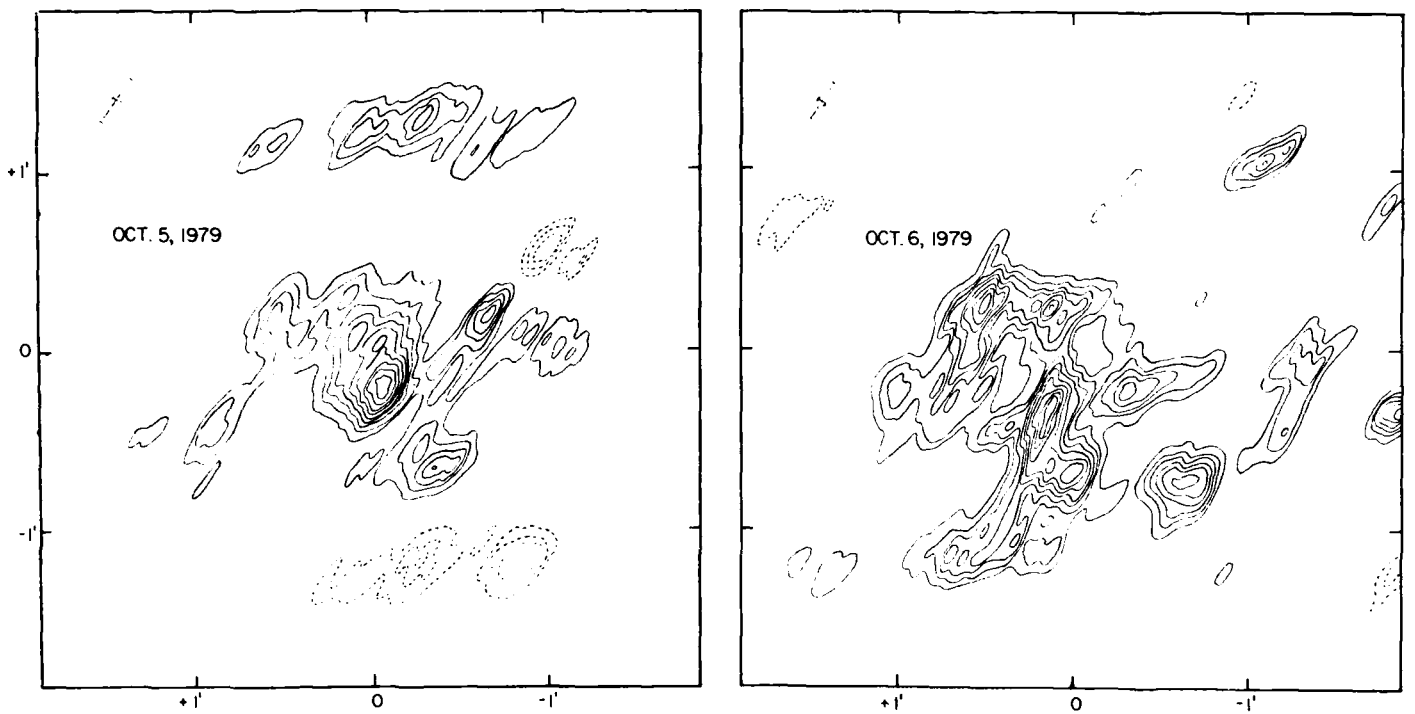

Figure 1. V.L.A. synthesis maps of the total intensity, I, at λ = 6 cm for AR 2032 on October 5 and 6, 1979. Here, the contours mark levels of equal brightness temperature corresponding to 0.1, 0.2...1.0 times the maximum brightness temperature of 1.95×10^6 K and 2.50×10^6 K respectively. Brightness temperatures of $\sim 10^6$ K indicate an origin in the solar corona, while the structural changes indicate an evolutionary time scale on the order of one day.

The synthesis maps obtained on the two days are quite different, indicating that the 6 cm emission from solar active regions can undergo significant structural changes on a time scale of one day. The lifetimes of the so-called "coronal condensations" and the bright chromospheric plage can also be measured in days, suggesting an intimate connection between these features and the radiation at centimeter wavelengths. In fact, comparisons of our total intensity maps with Hα photographs of the same regions indicate a detailed correlation between the regions of enhanced radio emission and the chromospheric plage seen as bright regions on the Hα photographs. The comparable angular resolutions and second-of-arc positional accuracy were in part due to accurate optical wavelength measurements of the sunspot positions which were made by Dr. Neidig during simultaneous observations at the Sacramento Peak Observatory. The data shown in Figures 2 and 3 indicate that small regions of bright plage are associated with enhanced radio emission, and that the structural changes seen at 6 cm wavelength are correlated with similar changes in the chromospheric plage. Not only is the radio emission dominated by a plage-associated component whose individual features are correlated with bright Hα emission; but there is also weak or undetectable radio emission from the regions which directly overlay sunspots. Two small ($\sim$ 10"), bright ($\sim 10^6$ K) radio sources are found on the outer edges of one sunspot (on October 6), however; it is likely that these sources are related to the strongly curved magnetic field lines found at the outer edges of sunspots.

Figure 2. A comparison of V.L.A. synthesis maps of the total intensity at λ = 6 cm (black contours) with H_α photographs of the same region taken on the same day (Oct. 5). There is an excellent correspondence between the enhanced radio emission and the chromospheric plage seen as bright regions on the photographs; while the two sunspots (dark spots on the edges of the bright region) exhibit weak or undetectable radio emission. The H_α photographs were taken at the λ 6563 Å Balmer line with a 10 inch evacuated refractor using SO1 51 Kodak film. These photographs were taken by the U.S. Air Force as part of the SOON system, and were kindly provided by Dr. Neidig of the Sacramento Peak Observatory. The angular scale of the V.L.A. map and the H_α photograph are the same, and it can be inferred from Fig. 1, which gives the extent of the radio emission of ~ 1'.

Figure 3. A comparison of V.L.A. synthesis maps of the total intensity at λ = 6 cm (black contours) with H_α photographs of the same region taken on the same day (Oct. 6). There is an excellent correspondence between the enhanced radio emission and the chromospheric plage seen as bright regions on the photographs; while the two sunspots (dark spots on the edges of the bright region) exhibit weak or undetectable radio emission. The H_α photographs were taken at the λ 6563 Å Balmer line with a 10 inch evacuated refractor using SO1 51 Kodak film. These photographs were taken by the U.S. Air Force as part of the SOON system, and they were kindly provided by Dr. Neidig of the Sacramento Peak Observatory. The angular scale of the V.L.A. map and the H_α photograph are the same, and can be inferred from Figure 1, which gives the extent of the radio emission of ~ 1'.

In Figures 4 and 5 we present the V.L.A. synthesis map of circular polarization, V, at 6 cm on October 6 and compare it to a magnetogram of the same region. (No magnetogram was available for October 5). Here, dark magnetogram areas refer to regions of negative magnetic polarity, and correspond to positive, left hand circular polarization (solid lines); whereas light magnetogram areas refer to regions of positive magnetic polarity and negative, right handed circular polarization (dashed lines). The comparison indicates that the bright plage-associated radio source has one dominant magnetic polarity, and that its magnetic structure is correlated with the longitudinal magnetic field seen on magnetograms of the lower lying photosphere. This provides additional evidence that the 6 cm maps of circular polarization act as coronal magnetograms which delineate regions of intense longitudinal magnetic fields (Lang and Willson, 1979, 1980). The degree of circular polarization, $\rho_c = V/I$, varies from 40% to 100% in different regions of the bright, plage-associated source, with its brightest features having the lower degree of circular polarization. The observed sense of circular polarization corresponds to the extraordinary mode of wave propagation. The fact that the brightest radio emission exhibits only one dominant magnetic polarity, which agrees with that of the longitudinal magnetic field in the regions away from the sunspots, indicates that bright radio emission at 6 cm wavelength is not, in this case at least, directly associated with the magnetic fields of sunspots. Instead, the circular polarization seems to mark the upward extension of the photospheric magnetic field into the low solar corona in regions between sunspots.

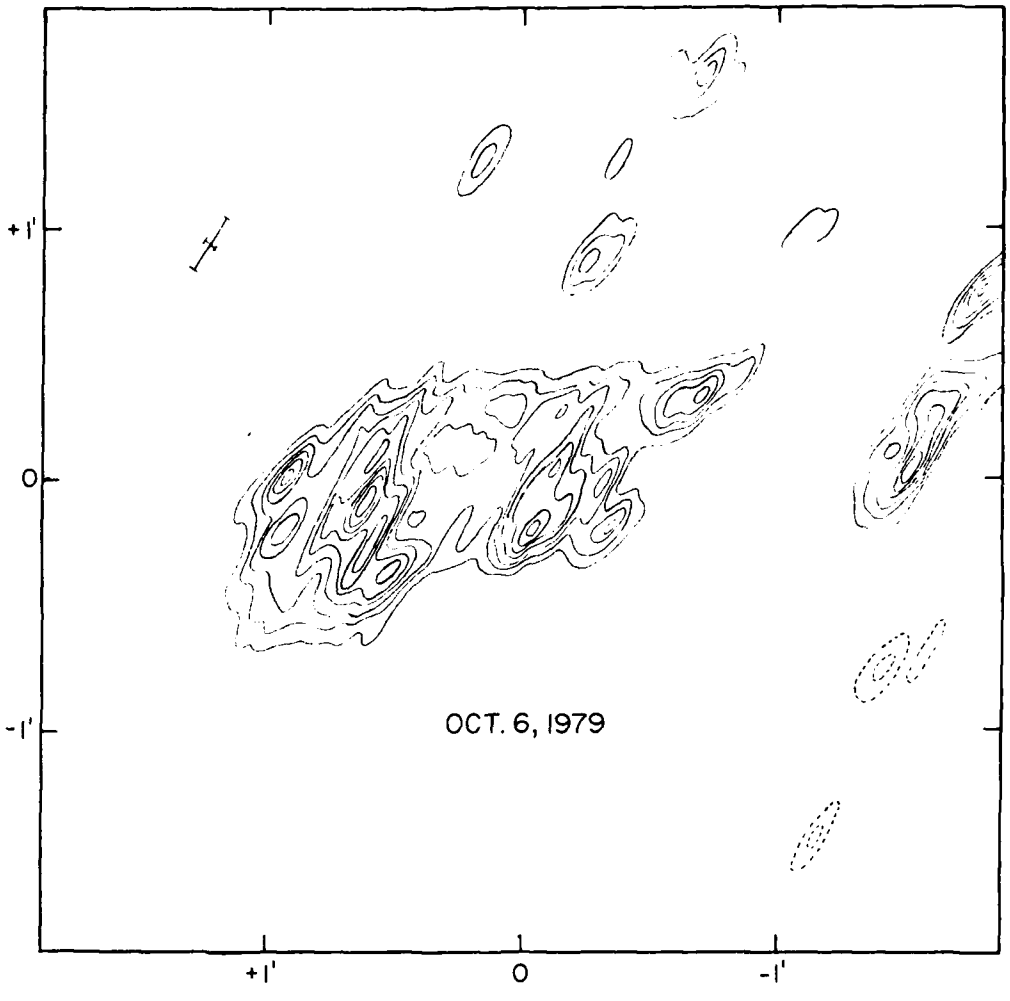

Figure 4. V.L.A. synthesis map of the circular polarization, or Stokes parameter, V, at λ = 6 cm for AR 2032 on Oct. 6, 1979. Here the contours mark levels of equal brightness temperature corresponding to 0.1, 0.2...1.0 times the maximum brightness temperature of 1.02×10^6 K. The ratio of the temperatures of the V and I maps indicate a degree of circular polarization, ρ_c = V/I, which ranges from 40% to 100% at different regions in the source.

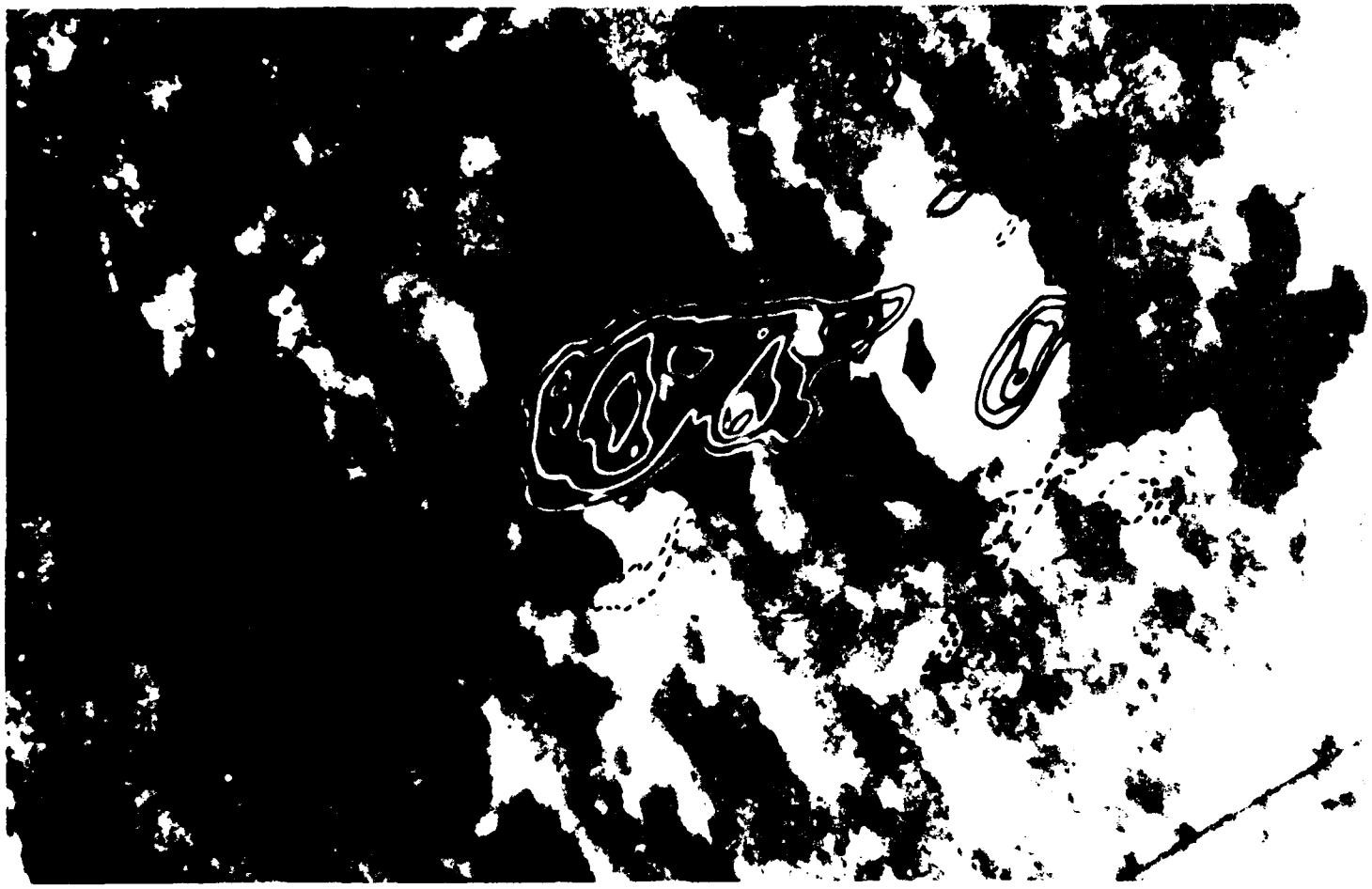

Figure 5. The V Map in Fig. 4 is compared with a Kitt Peak National Observatory (K.P.N.O.) magnetogram taken on the same day using Zeeman effect observations of the λ 8680 Å line of neutral iron. The circular polarization maps and the magnetograms respectively delineate the structure of the longitudinal component of the magnetic field in the corona and the photosphere. The magnetogram has been kindly provided by William Livingston of K.P.N.O., and it has an angular scale which is the same as that of the drawing superimposed upon it.

C. THEORETICAL DISCUSSION

The detailed correlation between the active region emission at Hα and 6 cm wavelengths (Figures 1 and 2), suggests that the dense chromospheric plage seen at Hα wavelengths extends vertically upwards into the solar corona where its hot ($\sim 10^6$ K) thermal radiation is detected as bremsstrahlung at 6 cm wavelength. The brightest features of the enhanced radio emission may have become optically thick, for their brightness temperatures, T_B, are about equal to the electron temperatures of $T_e = 2$ to 4×10^6 K which are known to exist in the coronal atmosphere above active regions. The larger part of the enhanced radio emission comes from optically thin regions with an optical depth $\tau = T_B/T_e \leq 1$, however; and we can use a representative optical depth of $\tau \sim 0.3$ to infer the average properties of the emitting region. Using the optical depth for bremsstrahlung (braking or free-free radiation) which applies at radio wavelengths for temperatures exceeding 3×10^5 K, we compute the emission measure, $\int N_e^2 d\ell$, of the radio emitting region using the relation (Lang, 1974b, 1980)

$$\int N_e^2 d\ell = \frac{102.19\ \tau\ \nu^2 T_e^{3/2}}{\ell n[4.7 \times 10^{10}\ (T_e/\nu)]} \approx 2 \times 10^{29}\ \text{cm}^{-5}, \qquad (1)$$

where the numerical value was obtained using our observing frequency of $\nu = 5 \times 10^9$ Hz, a representative electron temperature of $T_e = 2.5 \times 10^6$ K, and a representative optical depth of $\tau = T_B/T_e = 0.3$. This value of emission measure is consistent with those inferred from Skylab X-ray observations of the hot dense plasma distributed in coronal magnetic loops above other active regions. The X-ray observations indicate $T_e \tilde{\sim} 2.5 \times 10^6$ K and $\int N_e^2 d\ell \tilde{\approx} 2 \times 10^{29}$ cm^{-5} for the hot plasma trapped in magnetic arches above other active regions

(Landini, Fossi, Krieger and Vaiana, 1975; Vaiana, 1976; Vaiana, Krieger, Timothy and Zombeck, 1976; Vaiana and Rosner, 1978). Assuming that the vertical extent, L, of the radio emitting region is equal to the scale height at 10^6 K, we have $L \tilde{\sim} 10^{10}$ cm and an average electron density, $\bar{N}_e$, of

$$N_e = \left[\frac{\int N_e^2 d\ell}{L} \right]^{1/2} \tilde{\sim} 5 \times 10^9 \text{ cm}^{-3}. \quad (2)$$

Characteristic vertical extents of $L \tilde{\sim} 10^{10}$ cm and average electron densities of $\bar{N}_e \tilde{\sim} 5 \times 10^9$ cm^{-3} are also inferred from the Skylab X-ray observations. The data given in Section II also indicates that the observed brightness temperature immediately above sunspots is $T_B < 5 \times 10^4$ K, which for an electron temperature of $T_e = 2.5 \times 10^6$ K corresponds to an optical depth of $\tau < 0.02$, and from equation (1) and upper limit of $\int N_e^2 d\ell \sim 10^{28}$ cm^{-5} is obtained. This is also consistent with X-ray observations which indicate that the emission measure above sunspots is substantially lower than that above plage with emission measures characteristic of the quiet areas of the solar corona where $\int N_e^2 d\ell \sim 10^{27}$ cm^{-5} (Pallavicini, Vaiana, Tofani and Felli, 1979). In summary, then, the 6 cm radio emission of active region AR 2032 is dominated by a bright plage-associated source which can be explained in terms of the thermal bremsstrahlung of a hot, dense "coronal condensation"; and this interpretation leads to spatial configurations, emission measures, electron densities and temperatures which are consistent with those inferred from Skylab X-ray observations of the coronal atmosphere above other active regions.

The X-ray data indicate that the topological structure of the coronal magnetic fields largely determines the physical state of the dense coronal plasma, and we see the effects of these intense magnetic fields in the circular

polarization of the radio wavelength radiation. When a magnetic field is present, an electromagnetic wave is split into two normal waves, the ordinary, o, and extraordinary, e, waves; and the classical magneto-ionic theory can be used to calculate both the optical depths τ_o and τ_e for the two components and the degree of circular polarization, ρ_c, of the emergent radiation. As illustrated in Section II and by Lang and Willson (1980), the circularly polarized emission at 6 cm wavelength shows a strong correlation with the longitudinal magnetic fields seen on magnetograms, and we may therefore assume quasi-longitudinal propagation in which (Ratcliffe, 1962; Lang, 1974b, 1980; Krüger, 1979):

$$\tau_o = \frac{\tau}{[\,1 - (\nu_H/\nu)\,]^2}$$

$$\tau_e = \frac{\tau}{[\,1 + (\nu_H/\nu)\,]^2} \qquad (3)$$

and

$$\rho_c = \frac{\exp(-\tau_e) - \exp(-\tau_o)}{2 - [\exp(-\tau_o) + \exp(-\tau_e)]} \qquad (4)$$

where our observing frequency $\nu = 5 \times 10^9$ Hz, the gyrofrequency $\nu_H = 2.8 \times 10^6 H$ Hz for a longitudinal magnetic field of strength, H, and τ is the optical depth for thermal bremsstrahlung in the absence of a magnetic field. Optically thick bremsstrahlung with $\tau > 1$ is not polarized even in the presence of a magnetic field, and for optically thin bremsstrahlung with $\tau << 1$, equation (4) becomes

$$\rho_c \approx \frac{2\,(\nu_H/\nu)^2}{1 + (\nu_H/\nu)^2} \quad . \qquad (5)$$

Equations (3) and (4) indicate that lower polarizations are expected in the more intense regions where the optical depth τ approaches unity. This is in general agreement with our observation that the brightest features of the plage-associated source have the lowest polarization and may have become optically thick. The equations also indicate that the high observed circular polarizations of between 40% and 100% are possible in an optically thin plasma at frequencies ν near the gyrofrequency ν_H, and that the expected sense of polarization is that of the extraordinary wave. This sense of polarization is what is observed at both centimeter and millimeter wavelengths, but the high observed degrees of circular polarization at centimeter wavelengths require unusually high magnetic field strengths in the low solar corona. Magnetic field strengths of H = 450 to 900 Gauss are required at levels where the temperature exceeds 10^6 K if thermal bremsstrahlung accounts for the highly polarized radiation. In this situation the magnetic energy density of $H^2/(8\pi) \gtrsim 10^4$ erg cm^{-3} vastly exceeds the equipartition value inferred from the virial theorem, for the thermal kinetic energy density in the "coronal condensations" is $3N_e kT \sim 5$ erg cm^{-3}. It is no wonder, then, that the X-ray observations indicate that the dense, high temperature, coronal plasma is shaped by the coronal magnetic field. Moreover, as we shall see, the high magnetic field strengths inferred from the thermal bremsstrahlung hypothesis cannot be avoided by an appeal to the gyroresonant absorption hypothesis which requires absorption at the second or third harmonic of the gyrofrequency.

A comparison of the Skylab X-ray observations with 2.8 cm fan beam observations of comparatively coarse angular resolution (16" by 7') indicates

that regions of enhanced radiation at 2.8 cm wavelength are often associated with regions of enhanced X-ray emission located between sunspots (Pallavicini et al., 1979); and this component of the 2.8 cm radiation may also be interpreted in terms of the thermal bremsstrahlung of "coronal condensations". Other regions of enhanced 2.8 cm radiation occurred near sunspots where there is weak X-ray radiation, however, and this component may be related to the two small, bright 6 cm sources found at the outer edges of one sunspot in AR 2032. An alternative radiation mechanism is suggested in this case, where the thermal electrons may spiral about the intense magnetic fields of the sunspot; thereby giving rise to gyromagnetic processes which act as an additional source of opacity and circular polarization. These processes were used to explain the intensity and polarization spectrum of the slowly varying component in two-component, "core-halo" models incorporating gyroresonance absorption above sunspots and thermal bremsstrahlung in other regions (Zheleznyakov, 1962; Kakinuma and Swarup, 1962; Swarup et al., 1963; Lantos, 1968; Zlotnik, 1968a, b). Although the complete expression for gyroresonant absorption is somewhat complicated (Ginzburg 1961, 1967; Kakinuma and Swarup, 1962; Krüger, 1979), its basic properties can be inferred from the simplified optical depth formula which holds for quasi-longitudinal propagation with an index of refraction near unity (Zheleznyakov, 1970)

$$\tau = \frac{\pi \nu_p^2 L_H}{c\nu} \left(\frac{v_{th}}{c} \right)^{2n-2} \frac{n^{2n}}{n^{n+1} n!} (1 \pm \cos\theta)^2 \sin^{2n-2}\theta, \qquad (6)$$

or

$$\tau \approx 2.8 \times 10^{-13} N_e L_H \lambda \, (0.0344)^{2n-2} \frac{n^{2n}}{n^{n+1} n!} \, (1 \pm \cos\theta)^2 \sin^{2n-2}\theta, \qquad (7)$$

$$\approx 2 \times 10^{-15} N_e L_H \, (1 \pm \cos\theta)^2 \sin^2\theta \qquad \text{for } n = 2$$

$$\approx 3 \times 10^{-18} N_e L_H \, (1 \pm \cos\theta)^2 \sin^4\theta \qquad \text{for } n = 3$$

$$\approx 7 \times 10^{-21} N_e L_H \, (1 \pm \cos\theta)^2 \sin^6\theta \qquad \text{for } n = 4.$$

Here, the plasma frequency $\nu_p = 8.9 \times 10^3 N_e^{1/2}$ Hz for an electron density of N_e cm^{-3}, the thermal velocity $v_{th} = 6.5 \times 10^5 T^{1/2}$ at a temperature T, the factor $v_{th}/c = 0.0344$ for $T = 2.5 \times 10^6$ K, the observation wavelength is $\lambda = 6$ cm, the frequency ν is assumed to be at the n^{th} harmonic of the gyrofrequency ($\nu = n\nu_H$, n = 1, 2, 3...), the scale length of the magnetic field $L_H = H(dH/dz)^{-1}$ is the characteristic dimension for a change in magnetic field strength, H, with height, z, the angle between the line of sight and the direction of the magnetic field is denoted by θ, and the + and - signs respectively refer to the extraordinary and ordinary waves. Just as in the case of thermal bremsstrahlung, the extraordinary component of wave motion is more strongly absorbed; and it follows from Equations (4) and (6) that the degree of circular polarization, ρ_c, for the optically thin case ($\tau << 1$) becomes

$$\rho_c = \frac{2\cos\theta}{1 + \cos^2\theta} \, . \qquad (8)$$

For the conditions known to prevail in the solar atmosphere above active regions (N_e = 10^9 to 10^{10} cm^{-3}), and a reasonable assumption of L_H = 10^9 cm, equation (7) indicates that the gyroresonant absorption layers are normally opaque for n = 2, and that they are transparent for all $n \geq 4$. The optically thin condition required by the average observed brightness temperatures $T_B < T_e$ = 2 to 4 x 10^6 K and the high observed degrees of circular polarization ρ_c = 40% to 100% can be satisfied, however, for special conditions at the third harmonic of the gyrofrequency. Just as in the case of thermal bremsstrahlung, intense magnetic fields are required at levels where the electron temperatures are high, for the second and third harmonics of the gyrofrequency correspond to mangetic field strengths of H = 890 and 595 Gauss at our observing frequency of $\nu = n\nu_H$ = 5 x 10^9 Hz. The observed high degree of circular polarization is predicted by the gyroresonant absorption formulae, for equation (8) gives $\rho_c \geq 60\%$ for all θ smaller than seventy degrees. The expected brightness distribution is also a sensitive function of the angle θ, however, for the $\sin^{2n-2}\theta$ factor causes larger optical depths and hotter brightness temperatures at larger θ. The brightest polarized radiation is therefore expected in regions which are at large angles away from magnetic fields. This is inconsistent with our observations of the bright plage-associated component of AR 2032 whose emission is correlated with regions of intense longitudinal magnetic fields directed along the line of sight. The two small, bright radio sources found on the outer edges of one sunspot appear in regions where the line of sight is at large angles from the curved magnetic field lines of the sunspot, however; and these sources may well be due to gyroresonant absorption. We would, incidentally, expect that high

resolution observations of the sunspot-associated 2.8 cm emission will reveal intense sources at the outer edges of the sunspots.

An additional objection to the gyroresonant absorption process for the "coronal condensations" lying between sunspots is that it occurs in a thin layer of thickness (Lantos 1968)

$$D = \sqrt{\frac{2\pi}{3}} \quad \frac{v_{th}}{c} \quad L_H \cos\theta \lesssim 0.05\ L_H \lesssim 500 \text{ km.} \tag{9}$$

Gyromagnetic processes only become dominant in a very thin region above active regions, whereas thermal bremsstrahlung processes occur throughout the overlying solar atmosphere. For the conditions under consideration here, for example, we have $N_e = 5 \times 10^9$ cm^{-3}, $T_e = 2.5 \times 10^6$ K, $L_H = 10^9$ cm and $\nu = 5 \times 10^9$ Hz, which corresponds to an optical depth $\tau \geq 1$ at $n = 2$ and also at $n = 3$ for most θ. We might therefore imagine that radiation at the second or third harmonic of the gyrofrequency is completely absorbed in a thin layer above active regions, but that we actually observe the bremsstrahlung of the hot, dense gas which is known to overlay this thin layer in the so-called "coronal condensations". As shown in the preceding discussion, the bremsstrahlung from this higher lying coronal gas can account for both the observed brightness temperature and the observed circular polarization, and an appeal to gyromagnetic processes is unnecessary for the dominant plage-associated source seen at 6 cm wavelength. In the regions near sunspots where the coronal gas becomes more tenuous, we might expect to see the thin underlying gyroresonant layer; but only at special wavelengths corresponding to the condition that the observing frequency is at the second or third harmonic of the gyrofrequency. This special condition may

account for the fact that the sunspot-associated sources do not dominate the active region emission at 6 cm wavelength, when they do seem to dominate it in some cases at 2.8 cm wavelength.

D. CONCLUSIONS

We have compared the V.L.A. synthesis maps of the active region AR 2032 at 6 cm wavelength with Hα photographs and magnetograms with comparable angular resolutions and second-of-arc positional accuracy. The 6 cm emission is dominated by a small, bright source whose detailed morphological features are correlated with the chromospheric plage seen as bright regions on Hα photographs. This region of enhanced 6 cm emission exhibited substantial structural changes on a time scale of one day, and these changes were correlated with similar changes in the chromospheric plage. We interpret the observed emission of the bright plage-associated source in terms of the thermal bremsstrahlung of a hot ($T_e \gtrsim 2.5 \times 10^6$ K), dense ($\int N_e^2 d\ell \gtrsim 2 \times 10^{29}$ cm^{-5} and $N_e \gtrsim 5 \times 10^9$ cm^{-3}) "coronal condensation". The spatial configuration, emission measure, electron density and temperature are all consistent with those inferred from X-ray observations of the coronal atmosphere above other active regions. The plage-associated source is intimately associated with intense magnetic fields, for it is correlated with the longitudinal magnetic field, and a magnetic field strength of H = 450 to 900 Gauss is inferred from

the high degree of circular polarization. Our observations support the idea that the geometric arrangement of the coronal plasma is directly related to the surface structure of the solar magnetic field, and they suggest that the Sun's longitudinal magnetic field is vertically extended from the photosphere through chromospheric plage into the low solar corona. Weak or undetectable radio emission was found in the regions directly overlying sunspots, and this is compatible with X-ray and E.U.V. observations which indicate that a hot, dense plasma is located between groups of sunspots, and that cooler, tenuous regions overlay sunspots. Two additional small, bright 6 cm sources were found at the outer edges of one sunspot, however, and these sources could be due to gyroresonant absorption processes in the strongly curved magnetic fields at the outer edges of sunspots. Nevertheless, the brightest 6 cm emission of the active region comes from a hot, dense plasma located between sunspots; and this opens up the possibility that the previously unresolved core sources of the slowly varying S component are predominantly due to the thermal bremsstrahlung of the "coronal condensations" detected at X-ray wavelengths. Under this interpretation, the well-known correlation of the S component with groups of sunspots is simply due to the fact that the sunspots are part of active regions which contain a hot, dense thermal plasma which is trapped by intense magnetic fields which are not necessarily associated with the sunspots. Our observations indicate that it is this plasma which accounts for the large part of the enhanced radio emission at 6 cm wavelength, as well as the enhanced emission observed at X-ray wavelengths over active regions.

E. REFERENCES

Alissandrakis, C.E., Kundu, M.R. and Lantos, P. 1980, "A Model for Sunspot Associated Emission at 6 cm Wavelength", presented at I.A.U. Symposium No. 86: Radio Physics of the Sun.

Bracewell, R.N. (ed.) 1959, Paris Symposium on Radio Astronomy (Stanford: Stanford University Press).

Chiuderi Drago, F., Felli, M. and Tofani, G. 1977, Astron. Ap. 61, 79.

Chiuderi Drago, F., Fürst, E., Hirth, W. and Lantos, P. 1975, Astron. Ap., 39, 429.

Christiansen, W.N. and Mathewson, D.S. 1959, "The Origin of the Slowly Varying Component", in Bracewell (1959) p.108-117.

Christiansen, W.N., Mathewson, D.S., Pawsey, J.L., Smerd, S.F., Boischot, A., Denisse, J.F., Simon, P., Kakinuma, T., Dodson-Prince, H. and Firor, J. 1960, Ann. Ap., 23, 75.

Covington, A.E., 1949, Proc. I.R.E., 37, 407.

Denisse, J.F. 1950, Ann. Ap., 13, 181.

Felli, M., Pampaloni, P. and Tofani, G. 1974, Solar Phys., 37, 395.

Felli, M., Poletto, G. and Tofani, G. 1977, Solar Phys., 51, 65.

Felli, M., Tofani, G., Fürst, E. and Hirth, W. 1975, Solar Phys., 42, 377.

Foukal, P.V. 1975, Solar Phys. 43, 327.

Foukal, P.V. 1976, Ap. J., 210, 575.

Freidman, H. 1961, "X-ray and Extreme Ultraviolet Observations of the Sun", in Space Research II (ed. H.C. Van de Hulst, C. de Jager and A.F. Moore) (Amsterdam, North Holland). Reproduced in Lang and Gingrich (1979).

Gelfreich, G., Korol'kov, D., Rishkov, N. and Soboleva, N. 1959, "On the Regions Over Sunspots as Studied by Polarization Observations on Centimeter Wavelengths" in Bracewell (1959) pp 125-128.

Ginzburg, V.L. 1961, Propagation of Electromagnetic Waves in Plasma (New York: Gordon and Breach).

Ginzburg, V.L. 1967, Propagation of Electromagnetic Waves in Plasma 2nd Edition (New York: Gordon and Breach).

Ginzburg, V.L. and Zheleznyakov, V.V. 1959, Sov. Astron. A. J., 3, 235.

Kakinuma, T. and Swarup, G. 1962, Ap. J., 136, 975.

Krüger, A. 1979,Introduction to Solar Radio Astronomy and Radio Physics, (Boston: D. Reidel).

Kundu, M.R., 1959a, Ann. Ap., 22, 1.

Kundu, M.R., 1959b, "Etude Interferometrique des Sources d'Activite Solaire sur 3 cm de Longueur d'Onde", in Bracewell (1959), p.222-236.

Kundu, M.R. and Alissandrakis, C.E. 1975, Nature, 257, 465.

Kundu, M.R., Alissandrakis, C.E., Bregman, J.D. and Hin, A.C. 1977, Ap. J., 213, 278.

Kundu, M.R., Becker, R.H., and Velusamy, T. 1974, Solar Phys., 34, 185.

Kundu, M.R., and McCullough, T.P. 1972, Solar Phys., 24, 133.

Landini, M., Monsignori Fossi, B.C., Krieger, A. and Vaiana, G.S. 1975, Solar Phys. 44, 69.

Lang, K.R., 1974a, Solar Phys. 36, 351.

Lang, K.R., 1974b, Astrophysical Formulae (New York: Springer-Verlag).

Lang, K.R. 1980, Astrophysical Formulae 2nd Edition, (New York: Springer Verlag).

Lang, K.R. and Gingrich, O. 1979, A Source Book in Astronomy and Astrophysics 1900-1975 (Cambridge: Harvard University Press).

Lang, K.R. and Willson, R.F. 1979, Nature, 278, 24.

Lang, K.R. and Willson, R.F. 1980, "Very Large Array (V.L.A.) Observations of Solar Active Regions", in Radio Physics of the Sun: Proceedings of the I.A.U. Symposium No. 86 (Boston: D. Reidel).

Lantos, P. 1968, Ann. Ap. 31, 105.

Lehany, F.J. and Yabsely, D.E., 1949, Austr. J. Sci. Res. A2, 48.

Newkirk, G. 1961, Ap. J. 133, 983.

Pallavicini, R., Vaiana, G.S., Tofani, G. and Felli, M. 1979, Ap. J. 229, 375.

Piddington, J.H. and Minnett, H.C. 1951, Austr. J. Sci. Res. A4, 131.

Ratcliffe, J.A. 1962, The Magneto-Ionic Theory (Cambridge: Cambridge University Press).

Stepanov, K.N. 1958, Sov. Phys. J.E.T.P. 8, 195.

Swarup, G., Kakinuma, T., Covington, A.E., Harvey, G.A., Mullaly, R.F. and Rome, J. 1963, Ap. J. 137, 1251.

Tanaka, H. and Steinburg, J.L. 1964, Ann. Ap. 27, 29.

Vaiana, G.S. 1976, Phil. Trans. R. Soc. Lond. A281, 365.

Vaiana, G.S., Krieger, A.S., Timothy, A.F., and Zombeck, M. 1976, Astrophys. Space Sci. 39, 75.

Vaiana, G.S. and Rosner, R. 1978, Ann. Rev. Astron. Ap. 16, 393.

Waldemeier, M. 1956, Zeit. f. Ap. 40, 221.

Waldemeier, M. and Müller, H. 1950, Zeit. f. Ap. 27, 58.

Zheleznyakov, V.V. 1962, Sov. Astron. A.J. 6, 3.

Zheleznyakov, V.V. 1970, Radio Emission of the Sun and Planets (New York: Pergamon Press).

Zlotnik, E. Ya. 1968a, Sov. Astron. A.J. 12, 245.

Zlotnik, E. Ya. 1968b, Sov. Astron. A.J. 12, 464.